NANO LETTERS

2008
Vol. 8, No. 6
1746-1749

Observing Single Nanoparticle Collisions by Electrogenerated Chemiluminescence Amplification

Fu-Ren F. Fan and Allen J. Bard*

Department of Chemistry and Biochemistry, Center for Electrochemistry, The University of Texas at Austin, Austin, Texas 78712

Received April 1, 2008; Revised Manuscript Received May 1, 2008

ABSTRACT

We demonstrate a novel method of observing single particle collision events with electrogenerated chemiluminescence (ECL). A single event is characterized by the enhancement of ECL intensity during the collision of an individual platinum nanoparticle (Pt NP) on an indium tin oxide electrode, which catalyzes the oxidation of $Ru(bpy)_3^{2+}$ and a coreactant, for example, tri-*n*-propylamine (TPrA), present in the solution. Every collision produces a unique photon spike whose amplitude and frequency can be correlated with the size and concentration of the Pt NPs. A large amplification of ECL intensity can occur by choosing an appropriate measuring electrode and using high concentrations of $Ru(bpy)_3^{2+}$ and the coreactant.

We describe a novel method for observing the collisions of single conductive nanoparticles (NPs) at an electrode through measurement of light emission produced by electrogenerated chemiluminescence (ECL).[1] This can provide a useful approach to the study of electrochemical (EC) processes at single NPs, as well as the basis of highly sensitive electroanalytical methods. While most electrochemical research on NPs has focused on the properties of particle ensembles,[2–5] the exploration at the single particle level is also of interest. Experimental difficulties of a single NP usually involve problems in generating, locating, and characterizing a single particle, especially at the nanometer scale and in measuring the very small currents or charges associated, often only a few electrons, in electrode reactions at a single particle.[6] Several attempts have been made to amplify currents at ultramicroelectrodes (UMEs). For example, we trapped an ion in a nanometer-dimensional space between a nanometer diameter tip and a substrate and detected the current with the help of amplification due to a redox cycle.[7,8] Collinson and Wightman reported single electron transfer events by using ECL with very dilute solutions and a UME.[9] Aoki and Lei aimed at observed EC redox events at single 2.6 μm diameter latex particles coated with a 0.4 μm thick layer of polyaniline.[10] We have also recently demonstrated the possibility of observing single metal (Pt) NP collision events with a UME.[11] In this work a single collision event of a ~4 nm diameter particle was characterized by the current generated through a particle-catalyzed indicator reaction, for example, proton reduction, in the solution that occurs at the NP but not on the substrate UME. Since the indicator molecule can have a high concentration and a high diffusion coefficient, large amplification occurs.

Scheme 1

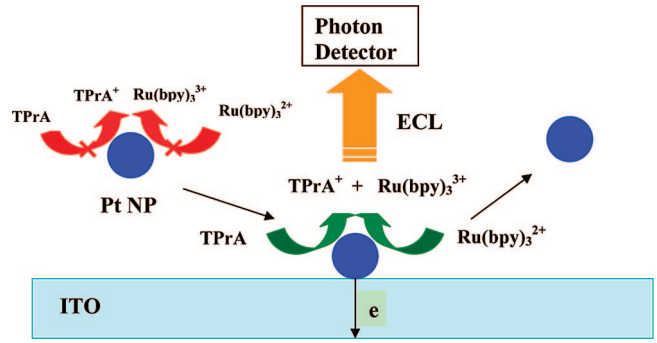

The method proposed here is related to this NP collision work and is based on the significant intensity amplification and fast temporal response of ECL involved in a rapid EC reaction of a species and its coreactant in single particle collision events. We use here the well-known ECL reaction based on the electrochemical oxidation of $Ru(bpy)_3^{2+}$ and TPrA.[1] In this system the oxidation produces $Ru(bpy)_3^{3+}$ and a radical from TPrA oxidation and deprotonation that react to produce $Ru(bpy)_3^{2+}$*. The reaction mechanism is complex and depends upon the nature of the electrode material.[12] The reactions of the species and the coreactant at relatively high concentrations in solution do not generate an appreciable ECL intensity at the conductive measuring electrode at a given potential (Scheme 1). For example, consider an indium tin oxide (ITO) electrode immersed in a solution of 2 nM Pt

* Corresponding author, ajbard@mail.utexas.edu.

10.1021/nl8009236 CCC: $40.75
Published on Web 05/21/2008

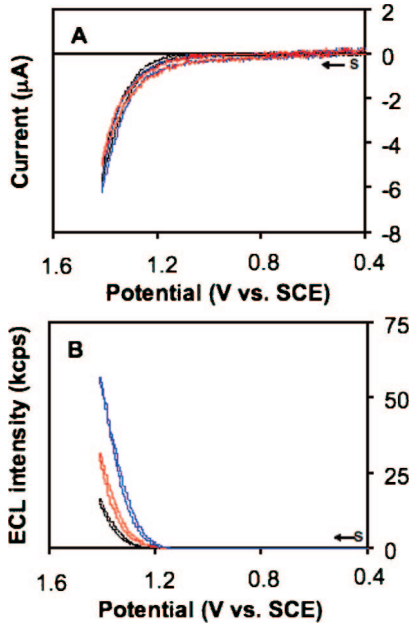

Figure 1. Cyclic voltammograms (frame A) and ECL intensity (kilocounts per second, kcps) vs potential curves (frame B) at an ITO electrode in a solution before (black curves) and after injecting 1 nM (red curves) and 2 nM (blue curves) Pt NPs. The solution contains 0.1 M $NaClO_4$, phosphate buffer (pH 7.0), 10 μM $Ru(bpy)_3(ClO_4)_2$, and 50 mM TPrA. Potential scan rate = 20 mV/s from point s.

NPs in 0.1 M $NaClO_4$ solution containing phosphate buffer (pH 7.0), 10 μM $Ru(bpy)_3^{2+}$, and 50 mM TPrA as a coreactant. The diffusion-controlled flux of particles to the surface of a planar macrodisk electrode, $J_{p,s}$, when the particles adhere to the surface, is given by

$$J_{p,s} = D_p C_p / \pi^{1/2} t^{1/2} \quad (1)$$

where D_p is the particle diffusion coefficient and C_p is the particle concentration. Ordinarily, in the simple NP or nanoelectrode charging process,[2,13] only one or a few electrons (n_p) would transfer between the NP and the electrode to yield a current, $i_{p,s} = n_p F A_e J_{p,s}$, that is much too small to observe above the background current level on a macroelectrode (where A_e is the electrode area and F is the Faraday). In the absence of Pt NPs as shown in the black curve of Figure 1B, no appreciable ECL intensity was observed until the electrode potential was slightly positive of 1.25 V vs SCE while significant current started to flow at potentials near ~1.0 V (see the black curve of Figure 1A). However if a NP is present and can electrocatalyze a reaction, species R to O (e.g., oxidation of TPrA) at a Pt NP upon its contact with the ITO, a significant enhancement in the ECL intensity as shown in the red curve of Figure 1B can be observed at lower bias potential (≤1.15 V), although no significant change in the current is found (see Figure 1A). Notice that the enhancement in ECL intensity, as shown in Figure 1B, increases with increasing concentrations of Pt NPs, indicating the enhancement is associated with an electrode reaction on the Pt NPs upon their contact with the ITO. As a control experiment we also carried out similar experiments with ITO NPs by using a Pt disk as the measuring electrode. In these experiments, we observed only a suppressed ECL intensity, although the background current increased substantially with the injection of ITO NPs into the test solution (see Figure S1 in the Supporting Information). Chen and Zu[14] observed a similar ECL intensity enhancement from an Au NP-coated ITO electrode as compared with a bare ITO electrode.

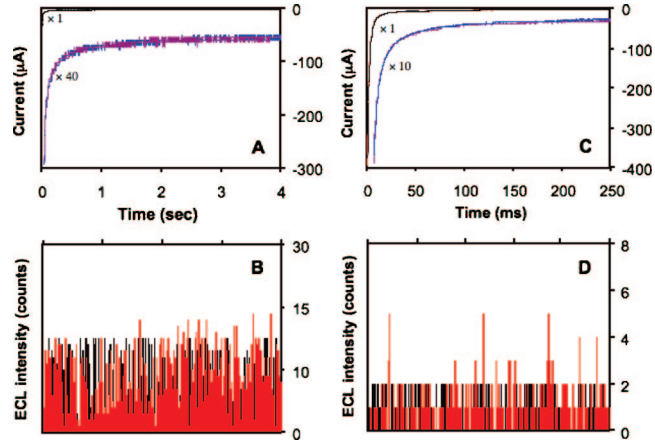

Figure 2. Current transients (frames A and C) and ECL intensity vs time records (frames B and D) at the ITO electrode before (black curves) and after (red curves) the injection of 2 nM Pt NPs colloidal solution. Current axis expansions (blue and violet curves): 40 times in frame A and 10 times in frame C. The solution contains 0.1 M $NaClO_4$, phosphate buffer (pH 7.0), 1.3 μM $Ru(bpy)_3(ClO_4)_2$, and 5 mM TPrA. Potential is stepped from 0 to 1.29 V vs SCE for 4 s (channel dwell (or binning) time, τ_{ch} = 15.6 ms) in frame B and for 250 ms (τ_{ch} = 975 μs) in frame D.

Figure 2 shows the current and ECL intensity transients at an ITO electrode in a solution before and after injecting Pt NPs.[15] In this set of experiments, we employed lower concentrations of redox species ($[Ru(bpy)_3^{2+}] = 2$ μM and [TPrA] = 5 mM) to decrease the background ECL intensity at ITO to more clearly observe the single ECL events.[16] As shown, the current transients (i vs t curves) before and after injection of the particle solution show smooth decay in both cases, while the ECL transients (I vs t curves) are stochastic. These current transients (see Figure 2A,C) are a result of double layer charging and the electrochemical oxidation of TPrA occurring at the measuring electrode with only a very small contribution from electron transfer associated with the NPs. In the diffusion controlled regime (e.g., at step potential $E_s \geq 1.5$ V vs SCE), the current first decayed exponentially with time, followed by a $t^{-1/2}$ Cottrell behavior.[17] ECL intensity transients, I vs t curves, in various time domains (from a few milliseconds to a few seconds) with or without added Pt NPs are compared and shown in Figure 2B,D. Additional I vs t curves are shown in the Supporting Information (Figure S2).

In the absence of Pt NPs, the ECL intensity transient, i.e. the I vs t profile, at a smaller bias, for example, E_s = 1.29 V vs SCE, the transient showed a rapid increase of ECL counts to reach a maximum within a few tens of milliseconds (~10 ms estimated from the black responses of Figure 2D); it then decayed slightly to a near steady state value with some fluctuation (see the black curves of Figure 2B,D). In the first few ms, no ECL counts could be recorded because of double layer charging prior to significant electron transfer processes. Particle collisions with the electrode typically give rise to different types of I vs t responses, as shown in the red

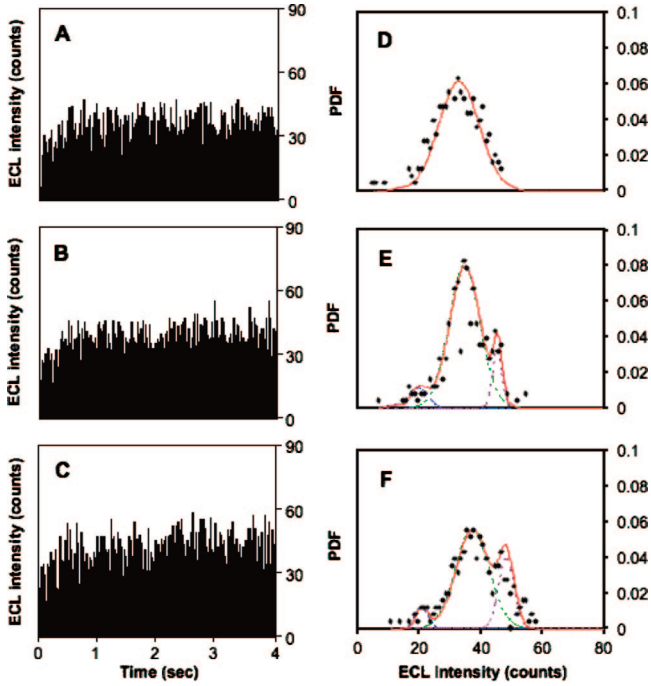

Figure 3. ECL transients (frames A, B, and C) and the corresponding probability distribution functions (PDFs) with decomposed multi-Gaussian distributions (frames D, E, and F) at three different concentrations of Pt NPs at an ITO electrode (A and D, no NPs; B and E, 1 nM Pt NPs; C and F, 2 nM Pt NPs). Potential is stepped from 0 to 1.29 V vs SCE for 4 s, and the solution contains 3 μM $Ru(bpy)_3(ClO_4)_2$, 5 mM TPrA, and PBS in 0.1 M $NaClO_4$ (pH 7.0).

trajectories in Figure 2B,D. Each I vs t profile is the combination of two ECL processes: one directly from the measuring ITO electrode and the other associated with individual single Pt particle collisions with the electrode. The overall I vs t profile in the presence of NPs is a transient similar to that when NPs are not present, superimposed with some large bursts of light. We attribute these large photon spikes (above the steady background) to the ECL events at single NPs. The frequency of the spikes depends strongly on E_s. We have examined this effect by setting the potential at even more positive values, where we observed more photon spikes. However, the current and ECL intensity decayed with time when the bias potential was >1.7 V. This may be caused by the deactivation of the ITO surface.

Both the overall ECL intensity and ECL transients associated with individual single particle collisions with the electrode will be affected by the concentration of NPs. Figure 3 shows the I vs t curves and the corresponding probability density functions (PDFs) and their decomposed multi-Gaussian distributions at three different NP concentrations. The PDF shows the probability that the data have a value (counts) within a defined range of counts at any given time.[8,18] In these experiments, the concentrations of $Ru(bpy)_3^{2+}$ and TPrA were kept constant at ($[Ru(bpy)_3^{2+}] = 3$ μM and [TPrA] = 5 mM), with NP concentrations of 0, 1, and 2 nM. In the absence of NPs, the total ECL intensity is 8248 counts after correction for the dark counts and the PDF is a single broad normal distribution having a mean, μ, of 33 counts and variance, σ, of 6.5 (see frame 3D). The addition of 1 nM Pt NPs into the solution increased the total ECL intensity to 9037 counts and the PDF could be decomposed into three normal distributions with individual μ at 20, 35, and 45 counts. With an increase of the Pt NP concentration to 2 nM, the total ECL intensity increased to 9788 counts. This concentration increase of Pt NPs did not significantly change the three μ values, but increased considerably the relative contribution of the peak at $\mu \approx 48$ counts and decreased that of the second peak at $\mu \approx 34$ counts to the overall ECL intensity. These results suggest that the contribution of the PDF peak at 33 to 35 counts to the ECL comes from the reactions occurring directly at the measuring ITO electrode, while the ECL peak at 45−47 counts is mainly associated with the reactions occurring at NPs when they collide with the electrode. The power spectral density function (PSDF),[8] (also called the frequency response function (FRF)) of the I vs t curves can be obtained by the Fourier transform of the time correlation function of the data. FRF of the ECL transient represents the fluctuation of ECL intensity in the frequency domain. The results for the time domain of 0−4 s in solutions with or without NPs are compared and shown in Figure S3C,D in the Supporting Information. Both contain a dominant dc component (0 Hz); however, in the presence of 2 nM Pt NPs, there are also significant contributions from higher frequency components at 6−32 Hz. At higher temporal resolution for ECL acquisition (see the ECL transient shown in Figure 2D for time domain of 0−250 ms), significant spike frequencies above the background ECL (i.e., when no Pt NPs are present in the solution) range from 35 to 450 Hz. These high-frequency ECL fluctuations can be attributed to Pt NPs and the ECL processes associated with individual particle collisions with the electrode.

The ECL intensity associated with individual single particle collisions with the electrode will be affected by the size of the NPs, the nature of the interaction between particle and the electrode surface (e.g., the particle residence time on or at the electrode surface), the concentrations and the electron transfer kinetics of indicator species and coreactant on NPs, and the lifetimes of active intermediate precursors and excited states. For example, if the particle sticks on the electrode, one should see a different behavior, as previously discussed for electrochemical mesasurements,[11] where a steady-state emission would follow the collision. At the other extreme, a single, noninteracting, collision should occur in a very short time, with relatively few photons emitted. Several combinations of the measuring electrodes and NP materials have also been examined. These results will be further addressed with additional experiments and analyses, and the results will be reported in the future.

In conclusion, we have demonstrated a novel method of observing single particle collision events with ECL. A single event is characterized by the ECL generated through the particle-catalyzed reactions of an indicator species and a coreactant present in the solution. Due to the fast temporal response, every collision produces a unique I vs t profile that is a function of the particle interaction with the electrode surface. In comparison to amplifying optical, conductivity,

and mass signals using nanoparticles,[19,20] the catalytic ECL amplification should allow a study of the dynamics of the process and information about the heterogeneous electron-transfer kinetics at the single particle level. Thus, in addition to the usual advantage of single particle studies compared to ensembles of obtaining information about particle environments, this approach may also provide dynamic information not seen in ensembles. Moreover, because of the high amplification found, it should be useful as a very sensitive analytical method, even down to the single molecule level.

Acknowledgment. The support of this research by The UT Center for Electrochemistry, BioVeris, Inc., and the Robert A. Welch Foundation is gratefully acknowledged. We are indebted to Dr. Xiaoyin Xiao for the synthesis and characterization of the Pt NPs.

Supporting Information Available: Additional CVs and ECL intensity figures. This material is available free of charge via the Internet at http://pubs.acs.org.

References

(1) *Electrogenerated Chemiluminescence*; Bard, A. J., Ed.; Marcel Dekker, Inc.: New York, 2004.
(2) Chen, S. W.; Ingram, R. S.; Hostetler, M. J.; Pietron, J. J.; Murray, R. W.; Schaaff, T. G.; Khoury, J. T.; Alvarez, M. M.; Whetten, R. L. *Science* **1998**, *280*, 2098–2101.
(3) Narayanan, R.; El-Sayed, M. A. *J. Phys. Chem. B* **2005**, *109*, 12663–12676.
(4) Harnisch, J. A.; Pris, A. D.; Porter, M. D. *J. Am. Chem. Soc.* **2001**, *123*, 5829–5830.
(5) Polsky, R.; Gill, R.; Kaganovsky, L.; Willner, I. *Anal. Chem.* **2006**, *78*, 2268–2271.
(6) Tel-Vered, R.; Bard, A. J. *J. Phys. Chem. B* **2006**, *110*, 25279–25287.
(7) Fan, F. R. F.; Kwak, J.; Bard, A. J. *J. Am. Chem. Soc.* **1996**, *118*, 9669–9675.
(8) Bard, A. J.; Fan, F. R. F. *Acc. Chem. Res.* **1996**, *29*, 572–578.
(9) Collinson, M. M.; Wightman, R. M. *Science* **1995**, *268*, 1883–1885.
(10) Aoki, K.; Lei, T. *Langmuir* **2000**, *16*, 10069–10075.
(11) Xiao, X.; Bard, A. J. *J. Am. Chem. Soc.* **2007**, *129*, 9610–9612.
(12) Zu, Y.; A. J. Bard, A. J. *Anal. Chem.* **2000**, *72*, 3223.
(13) Fan, F. R. F.; Bard, A. J. *Science* **1997**, *277*, 1791–1793.
(14) Chen, Z.; Zu, Y. *Langmuir* **2007**, *23*, 11387–11390.
(15) Briefly, the Pt colloidal solution was obtained by reducing 2 mM H_2PtCl_6 with sodium borohydride in the presence of sodium citrate (ref 11). The particle sizes ranged between 2 and 6 nm distributed mainly at 4 ± 0.8 nm in diameter.[11] Assuming a particle contains about 2000 Pt atoms, the stock solution was about 1 μM in particles. Before each experiment, the as-prepared Pt colloidal stock solution was diluted 10 times with water. A few to 100 μL of this solution was injected into about 5 mL test electrolyte in the electrochemical cell yielding a particle concentration in the test solution in the pM to nM range after mixing the solutions. The current and ECL intensity vs time responses were recorded upon stepping the potential to a desired value. The ITO electrode area was $\sim$0.07 cm^2.
(16) The single photon counting technique used for ECL event recording has recently been described in Figure 33, Chapter 2 of ref 1, with some modifications. The active area of the photon detector is $\sim 7.5 \times 10^{-5}$ cm^2. More detailed description for the schematics of the arrangement of ITO electrode and optical system is described in Figure S4 in the Supporting Information.
(17) Bard, A. J.; Faulkner, L. R. *Electrochemcial Methods, Fundamentals and Applications*, 2nd ed.; John Wiley & Sons: New York, 2001.
(18) Bendat, J. S.; Piersol, A. G. *Random Data Analysis and Measurement Procedures*, 2nd ed.; John Wiley and Sons: New York, 1986.
(19) Sonnichsen, C.; Reinhard, B. M.; Liphardt, J.; Alivisatos, P. A. *Nat. Biotechnol.* **2005**, *23*, 741–745.
(20) Zhang, Z. L.; Pang, D. W.; Yuan, H.; Cai, R. X.; Abruna, H. *Anal. Bioanal. Chem.* **2005**, *381*, 833–838.

NL8009236